# *Software Package for 3 Dimensional Non-Linear Elastic Analysis of Caverns*

***N. K. Samadhiya***
***M. N. Viladkar***
*&*
***Pradeep Bhargava***

*Department of Civil Engineering,*
*Indian Institute of Technology Roorkee,*
*Roorkee-247 667, India*
*Ph.: +91-01332-285467 Fax : +91-01332-273560*
*Email: nksamfce@iitr.ernet.in*

**ABSTRACT**

The finite element method of analysis is one of the several well-developed numerical techniques that can provide useful information for engineering surface and underground excavations in rock. Its application to design in civil and mining engineering projects is essentially an analysis of displacements that leads to estimates of changes in stresses and strains induced during excavation process. There is a great generality in terms of handling the problems having a complex geometry involving layered, non homogeneous rock masses and possible supporting structures interacting with them. Most of the studies carried out so far are, which can be simulated as a 2 D plane strain problem, essentially for assessing the stability of tunnels. However, for an accurate and robust prediction of the structural behaviour of the cavern/ large underground opening, a complete three dimensional finite element analysis is required. Though the efforts required in mesh generation for heterogeneous domain for a 3 D analysis are enormous, nevertheless it enables the designer to solve the problems posed by EGO (Extraordinary Geological Occurrences), which are very common in the geologically complex Himalaya.

The paper deals with the development of a software package for 3-dimensional analysis of stresses in anisotropic rock masses named as ASARM. The software is capable of taking into account in-situ stresses, anisotropy (inherent and induced) and stress dependent modulus. Three typical problems have been analysed to validate the software.

***Keywords:*** Finite element method, numerical techniques, underground excavations, stability, heterogeneous, stresses, strains

## 1. INTRODUCTION

A number of hydroelectric projects are in design and construction stage in India for utilising untapped hydro energy. The construction of large caverns for powerhouses, particularly in complex geological conditions, is a new challenge. The behaviour of the caverns in massive competent rock, although complicated, has already been studied using theories of elasticity, plasticity and rheology. The behaviour is further complicated by the complex geological conditions such as, presence of joints and shear zones. Under similar complex geological conditions powerhouse caverns of Sardar Sarovar Multipurpose Project, Tehri Hydro Development Project and Nathpa Jhakri Power Project are under construction in India.

Limitations of the physical - geomechanical models of hydroelectric projects motivated the research workers in the early 70s to develop empirical models based on field observations and case histories. Later, with the realization of limitations of the empirical models and advent of personal computers, research efforts were directed towards several numerical techniques, e.g,. the finite element method (FEM), the boundary element method (BEM) and the distinct element method (DEM). Out of these, FEM has emerged as the most popular technique among civil engineers due to its generality and ability to model rock mass discontinuities and the associated anisotropy.

Review of the literature suggests that the analysis and design of caverns is generally based upon 2-D linear elastic finite element analysis. The general approach, is to assume reduced modulus of deformation and perform analysis considering the rock mass as isotropic if the joint sets are three plus or random or both and there is no major shear zone. However, it is a gross simplification if the presence of one joint set with or without a major shear zone is ignored and the rock anisotropy is not considered in the analysis. An accurate and realistic prediction of the structural behaviour of cavern requires three dimensional finite element analysis to consider the effect of complex geological features such as shear zones and major discontinuities and intrusions.

In the present study, a software package, for 3-D non-linear elastic analysis of stresses in anisotropic rock masses (ASARM) has been developed using finite element method with the capabilities to simulate in-situ stresses and geological discontinuities like shear zones, fault zones and anisotropy associated with jointed rock masses. The nonlinear elastic analysis is justified when the caverns are located in the non-squeezing rock mass.

In order to simulate the major discontinuities in a cavern, like shear zones, a generalised three-dimensional joint / interface element has been incorporated in the software to model interface of jointed rock mass and shear zone taking into consideration the dilatancy, roughness and undulating surface of a discontinuity.

The constitutive equations, proposed by Samadhiya (1998), to account for the complex anisotropy of the rock mass according to its micro-structural nature have been incorporated in the program. The compliance matrix of the rock mass is assumed as equal to the sum of compliance matrices of the isotropic rock material and all the joint sets.

## 2. FINITE ELEMENT FORMULATION

In the finite element method, the domain of interest is first subdivided into a number of discrete sub-domains or elements. Over an individual finite element, the behaviour, in the present case the deformations in the continuum, is approximated from the nodal values using the pre-established shape functions defined within a given element. Once the behaviour of the domain has been represented in terms of the discrete nodal values, technique like the weighted residual method, virtual work statement or variational methods (Bathe, 1982; and Zienkiewicz & Taylor, 1992) form the basis for the finite element formulation. The outcome is a discretized equilibrium expression which, is turn, when combined with the constitutive equation, results in a set of equations which are, finally, solved for the unknowns like displacements from which strains and stresses can be computed.

### 2.1 Element Geometry

In the present study, the hexahedral continuum element has been employed for the finite element discretization. As is well known in finite element literature, the discretization would enable the element geometry in terms of (x, y, z) co-ordinates of a point to be written as

$$x = \sum_{i=1}^{n} N_i(\xi,\eta,\zeta)\ x_i$$

$$y = \sum_{i=1}^{n} N_i(\xi,\eta,\zeta)\ y_i$$

$$z = \sum_{i=1}^{n} N_i(\xi,\eta,\zeta)\ z_i \qquad (1)$$

where n is the number of nodal points in an element (20 in the present case for rock mass element and 16 for joint element).

$N_i$ is the standard iso-parametric shape function, mapping a bi-unit cube in ($\xi$, $\eta$, $\zeta$) space to a general hexahedron in (x , y, z) space, which for corner nodes can be defined as

$$N_i = \frac{1}{8}(1+\xi\xi_i)(1+\eta\eta_i)(1+\zeta\zeta_i) \qquad (2a)$$

and for mid side nodes along $\xi = 0$ plane as

$$N_i = \frac{1}{4} (1 - \xi^2) (1 + \eta\eta_i) (1 + \zeta\zeta_i) \quad (2b)$$

along $\eta = 0$ plane as

$$N_i = \frac{1}{4} (1 - \eta^2) (1 + \xi\xi_i) (1 + \zeta\zeta_i) \quad (2c)$$

and along $\zeta = 0$ plane as

$$N_i = \frac{1}{4} (1 - \zeta^2) (1 + \xi\xi_i) (1 + \eta\eta_i) \quad (2d)$$

where $\xi_i$, $\eta_i$, $\zeta_i$ are the co-ordinates of the $i^{th}$ node of the bi-unit cube.

## 2.2 Element Kinematics

The basic kinematic variable occurring in the present formulation is displacement defined through its components u, v, w (grouped in vector {u}) in the direction of the reference system axes (x , y, z). Like geometry, the displacement variation within the element may be uniquely related to nodal displacements, $\{\delta_e\}$, through the shape function matrix $[N_i]$ as

$$\{u\} = \left[N_i (\xi, \eta, \zeta)\right] \{\delta_e\} \quad (3)$$

where $\{u\} = \{u, v, w\}^T$ (3a)

$$\{\delta_e\} = \{u_1 , v_1 , w_1 ,..., u_n , v_n , w_n \}^T \quad (3b)$$

$$[N] = [N_1 \mathbf{I}, N_2 \mathbf{I}, N_3 \mathbf{I},\ldots,N_n \mathbf{I}] \quad (3c)$$

n = number of nodes in the element

and $$[\mathbf{I}] = \begin{bmatrix} 1 & 0 & 0 \\ 0 & 1 & 0 \\ 0 & 0 & 1 \end{bmatrix} \quad (3d)$$

The strain components are obtained as derivatives of the displacement variable as,

$$\{\varepsilon\} = [L] \{u\} \quad (4)$$

where, $\{\varepsilon\} = \{\varepsilon_x , \varepsilon_y , \varepsilon_z , \gamma_{xy} , \gamma_{yz} , \gamma_{zx} \}^T$ (4b)

and L is the linear differential operator for small strains which is defined as

$$[L] = \begin{bmatrix} \frac{\partial}{\partial x} & 0 & 0 \\ 0 & \frac{\partial}{\partial y} & 0 \\ 0 & 0 & \frac{\partial}{\partial z} \\ \frac{\partial}{\partial y} & \frac{\partial}{\partial x} & 0 \\ 0 & \frac{\partial}{\partial z} & \frac{\partial}{\partial y} \\ \frac{\partial}{\partial z} & 0 & \frac{\partial}{\partial x} \end{bmatrix} \tag{4b}$$

Combining Eqs. 3 and 4 enables the discretized strain - displacement relation to be expressed as,

$$\{\varepsilon\} = [L]\,[N]\,\{\delta_e\} = [B]\,\{\delta_e\} \tag{5}$$

where,

$$[B] = \begin{bmatrix} [B_1] & [B_2] & [B_3] & \cdots [B_n] \end{bmatrix} \tag{5a}$$

and

$$[B]_i = \begin{bmatrix} \frac{\partial N_i}{\partial x} & 0 & 0 \\ 0 & \frac{\partial N_i}{\partial y} & 0 \\ 0 & 0 & \frac{\partial N_i}{\partial z} \\ \frac{\partial N_i}{\partial y} & \frac{\partial N_i}{\partial x} & 0 \\ 0 & \frac{\partial N_i}{\partial z} & \frac{\partial N_i}{\partial y} \\ \frac{\partial N_i}{\partial z} & 0 & \frac{\partial N_i}{\partial x} \end{bmatrix} \tag{5b}$$

### 2.3 Constitutive Relation

The elastic stress-strain relation for a three-dimensional continuum may be expressed in the usual matrix form

$$\{\sigma\} = [D]\,\{\varepsilon\} + \{\sigma_o\} \tag{6}$$

where, [D], the elasticity matrix for anisotropic rock masses,

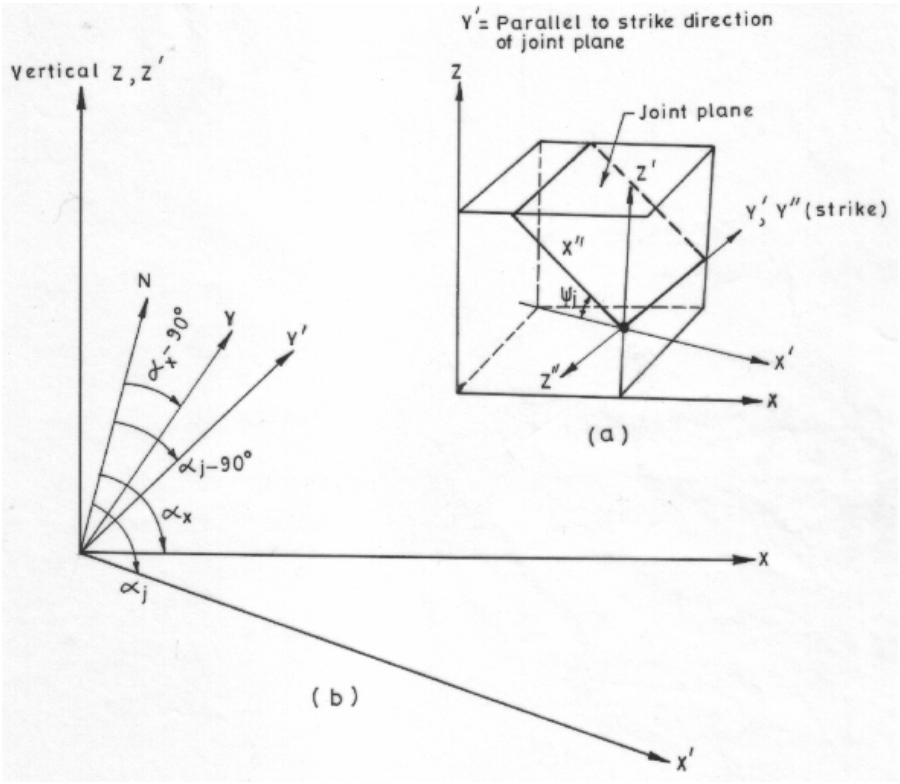


Fig. 1 - Rotation of axes

$\{\varepsilon\}$ = Strain

$\{\sigma_o\}$ = Insitu stresses.

### *2.3.1 Constitutive law for jointed rock mass*

Figure 1 shows axes system for resolution of stresses along a joint plane. The stress $\{\sigma\}$ are resolved to X', Y', Z' axes system i.e. $\{\sigma'\}$ which then are further resolved to X", Y", Z" system $\{\sigma"\}$ in order to get stresses perpendicular to joint plane and in joint plane in orthogonal directions (Fig. 2). The corresponding transformation matrices $\left[D_j^{'}\right]$ and $\left[D_j^{"}\right]$ comprise of respective direction cosines. Finally, stresses on the joint plane are obtained as

$$\{\sigma"\} = [D_j^{"}]\,[D_j^{'}]\,\{\sigma\} \qquad (7)$$

Samadhiya (1998) has proposed elastic constitute equations based on an equivalent material approach. It aims to capture the overall behaviour of the rock mass based on the constitute characteristics of intact rock and rock joints including their spacing and

orientation. The elasticity matrix of the jointed rock mass has been derived from the compliance matrix which in turn is obtained by integrating the compliances of the rock material and that of all the joint sets. The compliance matrices are transformed into global system before being summed up. The total strain in the rock mass is the sum of strains contributed by various joint sets.

The overall strain matrix (compliance matrix) of the jointed rock mass is given as

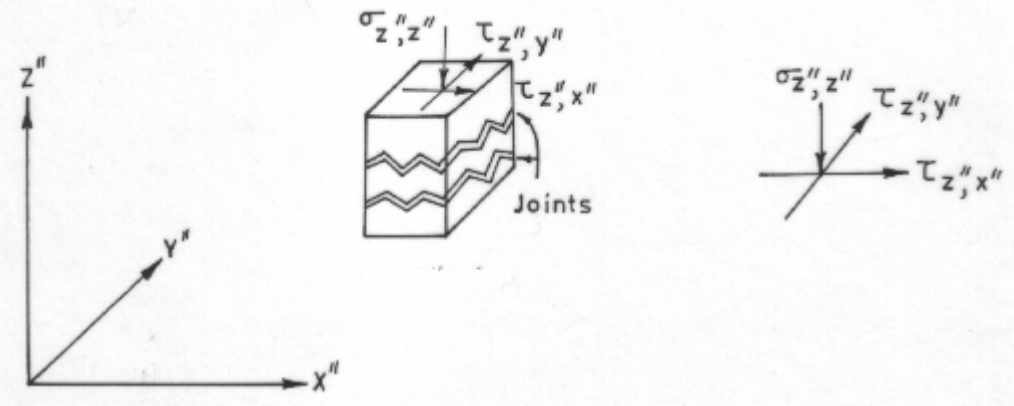


Fig. 2 - Stresses on joint plane

$$[H] = [H_r] + \sum_{j=1}^{n_j} [D_j^{''}]^T [H_j][D_j^{''}][D_j^{'}] \quad (8)$$

where

$[H_r]$ = compliance matrix of the rock material

$[H_j]$ = compliance matrix of the joint set

$[D_j^{'}]$ = first transformation matrix for resolving stresses from global X, Y, Z axes to X', Y' and Z'.

$[D_j^{''}]$ = second transformation matrix for resolving stresses from global X', Y', Z' axes to X'', Y'' and Z''.

$n_j$ = number of joint sets

Following parameters are required for a complete description of the constitutive relationship of material:

i) $E_r$ (elastic modulus) and $\nu_r$ (Poisson's ratio) of the rock material,
ii) Number of joint sets, their orientation (dip and dip direction) and joint frequency,.
iii) Normal stiffness ($k_n$ ) and shear stiffness ($k_s$ ) measured parallel to the joint surface for each joint set.

The above parameters would enable obtaining the elements of compliance matrices of a jointed rock mass. The inverse of the compliance matrix would give the [D] matrix.

### *2.3.2 Constitutive law for joint element/interface*

Goodman et al. (1968) provided the explicit element stiffness matrix, for use in a finite element analysis of a four noded rectangular joint element having zero thickness by minimising the energy equation with respect to the nodal displacements.

A generalised formulation of a three dimensional joint/interface element has been derived by Samadhiya (1998) to account for dilatancy, roughness and undulating surface of discontinuities. Figure 3 shows an isolated element alongwith its node numbers. Figure 4 represents the middle surface of the joint element at $\zeta = 0$ plane. The nodes coincide with the corresponding nodes on the top and bottom planes.

The strain $\{\varepsilon\}$ at any point in the joint element may be defined by the local tangential and normal relative displacement with respect to the plane of discontinuity. The interface stresses are then determined by multiplying the strain with the stress-strain matrix [D]. A detailed derivation of the rotation matrix [R] is given in the Ph.D. thesis of Samadhiya (1998).

## 2.4 Equilibrium

It is well known in finite element literature that the principle of virtual work provides a basis for the derivation of equilibrium statement. In the present context, it may be expressed as the balance between the virtual work due to external forces {F} and the internal virtual work due to stresses $\{\sigma\}$ integrated over the current volume. For a given element, the virtual work equation may be written as

$$\int \left\{\varepsilon_e^*\right\}^T \{\sigma_e\} dV_e - \left\{\delta_e^*\right\}^T \{F_e\} = 0 \qquad (9)$$

where, $\{\varepsilon^*\}$and $\{\delta^*\}$ are the virtual strain and displacement fields respectively.

On substitution of the strain - displacement relation in the above equation and noting that the expression must hold good for any arbitrary set of virtual displacements, the descretized equilibrium equation becomes:

$$\int_{Ve} [B]^T \left\{\sigma_e\right\} dV_e - \left\{F_e\right\} = 0 \qquad (10)$$

The above integral is evaluated through the Gauss-Legendre quadrature rule. The integral is made equivalent to the summation of integrand evaluated at Gauss integration points within the element multiplied by the corresponding weights.

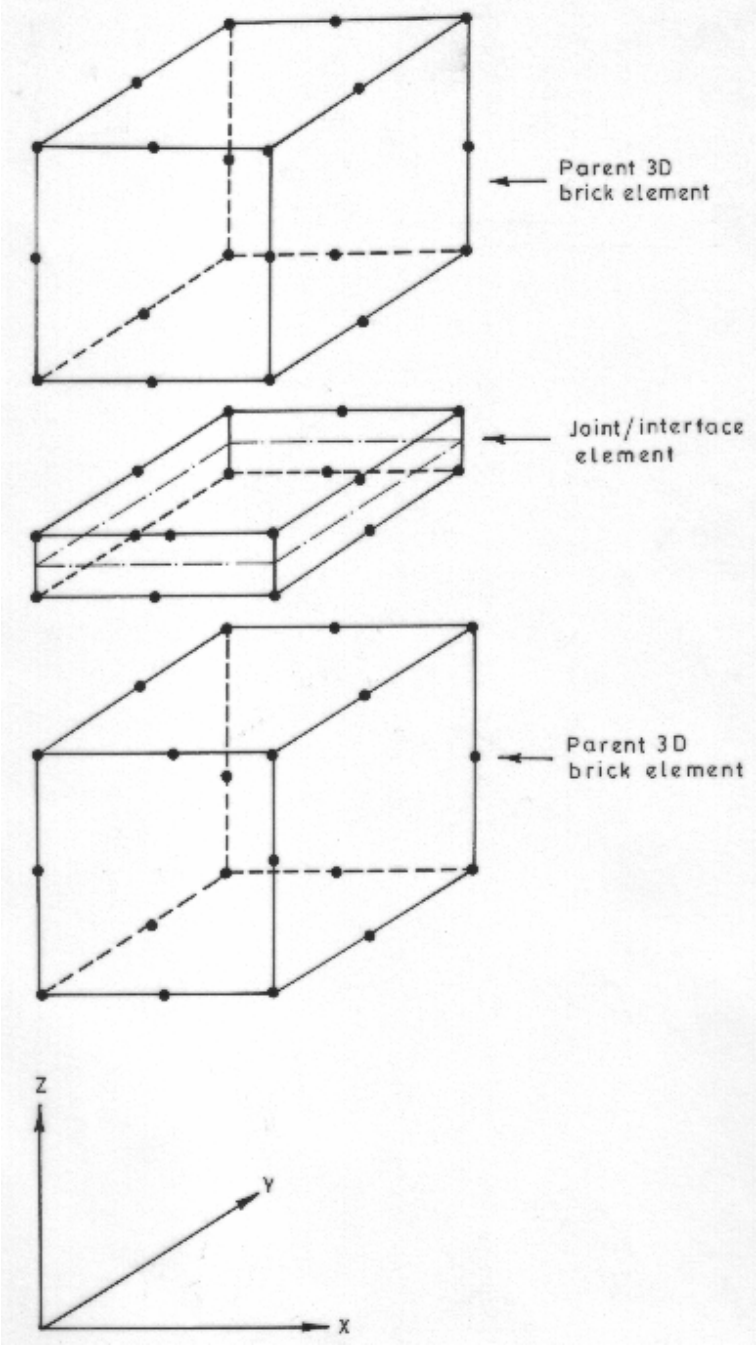


Fig. 3 - Joint/interface element sandwiched between two parent brick elements

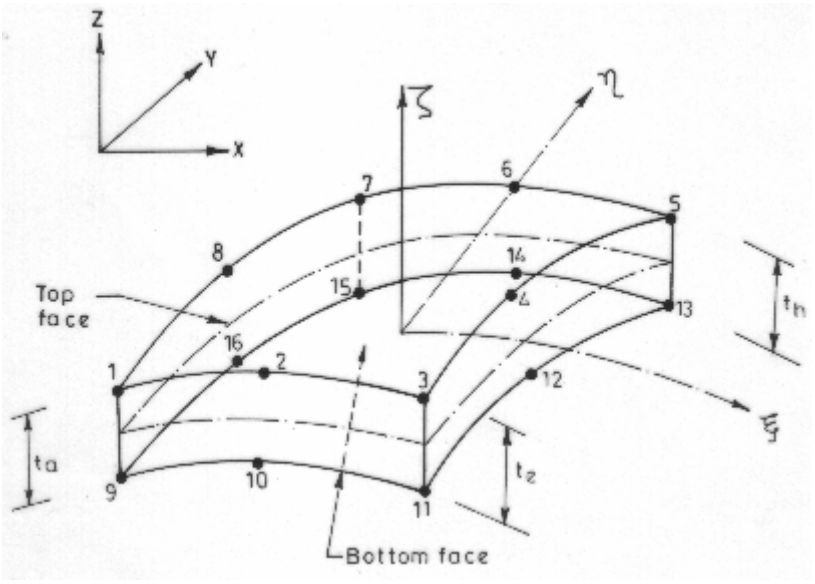


Fig. 4 - Isolated joint/interface element with nodal numbers and local axes

Now, taking into account the stress-strain law, and the compatibility equation, the equilibrium equation for an element is obtained as,

$$[K_e]\ \{\delta_e\} = [F_e] \tag{11}$$

where the stiffness matrix $[K_e]$ is given as,

$$\left[K_e\right] = \int_{V_e} [B]^T\ [D]\ [B]\ \ dV_e \tag{12}$$

The load vector includes the external loads applied to the system, e.g., concentrated loads, pressure and gravity loading. In addition, this load vector also requires an evaluation of the nodal forces due to stress release caused by the removal (or excavation) of a portion of the domain.

The nodal forces equivalent to the boundary tractions i.e. pressure loading {p} and the gravity loading {b} (body forces) may also be calculated by applying the principle of virtual work. These are given as the following equations:

$$\left\{F_b\right\} = \int_{V_e} [N]^T \{b\}\, dV_e \tag{13}$$

and $$\{F_p\} = \int_{A_e} [N]^T \{p\}\, dA_e \quad (14)$$

where, {b} and {p} are the body forces and pressure loading respectively. $[N]^T$ and $A_e$ are shape functions and area of the surface on which external tractions are applied.

Invariably, in-situ stresses within the rock continuum play a key role in the analysis, especially when stress dependent modulus is used. The in-situ stresses have been accounted for by applying them as initial stresses. However, in the excavated portion, no in-situ stresses are present, and therefore, the effect of the same need to be accounted for. In-fact, to obtain the displacements occurred due to release of in-situ stresses and further the resulting redistribution of stresses is the aim of entire analysis.

For that, load vector due to in-situ stresses in each element is calculated first, as

$$\{F_{eo}\} = \int_V [B]^T \{\sigma_0\}\, dV \quad (15)$$

where,

$$\{\sigma_0\} = \{\sigma_{x0}, \sigma_{y0}, \sigma_{z0}\}^T = \{K_x \gamma z, K_y \gamma z, \gamma z\}^T \quad (16)$$

in which $K_x$ and $K_y$ are the in-situ stress coefficients, $\gamma$ is the density of rock mass and z is the depth of Gauss point below ground surface.

It may be mentioned that actual in-situ stress (initial stress field) has been considered which is a better representation of the in-situ condition in comparison to $K_0$- condition. The shear components of the in-situ stress field have not been accounted for. However, in the case of steeply inclined ground surface, the stresses and displacements may be greatly influenced by these stresses.

This calculation is not carried out for the elements which fall in the excavated zone. The equivalent load vectors due to initial stresses are then added for all elements with reversed sign to obtain the global load vector due to initial stresses. This load vector contains non zero loads only on the excavated surface, as at all other nodes, loads from adjoining elements equalise each other. This process allows any element to be declared as excavated easily.

The stiffness matrix of the entire finite element mesh is obtained by assembling the contributions of all elements. This is done by adding together the contributions of each finite element to the force balance equations at the corresponding degrees of freedom. This process leads to the following global system of linear simultaneous equations.

$$[K]\ \{\delta\} = \{F\} \quad (17)$$

where, [K] is the global stiffness matrix of the assembled structure, $\{\delta\}$ is the nodal displacement vector and {F} is the load vector.

## 3. NON-LINEAR ELASTIC STRESS ANALYSIS

In general, two types of non-linearity can be present in a system, viz., i) due to material non-linearity and ii) due to geometric non-linearity. In both the cases, the finite element method can be applied to obtain a solution of the corresponding non-linear problem. Since the geometric non-linearity is of minor importance in underground openings, only non-linear material behaviour has been considered. To this end, a non-linear elastic stress analysis has been carried out wherein stress dependent elastic modulus (Janbu, 1963) has been employed in the constitutive equations, which may be written as,

$$\{\sigma\} = [D_\sigma]\ \{\varepsilon\} + \{\sigma_0\} \tag{18}$$

$[D_\sigma]$ is obtained by modifying [D] matrix to account for increased modulus of rock material and stiffness due to confinement. The following equation has been used to include the effect of pressure dependency.

$$E_r = E_o \left[\frac{\sigma_2 + \sigma_3}{2P_a}\right]^\alpha \tag{19}$$

where,

$E_r$ = pressure dependent modulus of the rock,

$E_o$ = modulus of deformation corresponding to unit pressure (which may be taken to be approximately equal to the modulus of deformation from uniaxial compressive strength tests),

$\sigma_2$, $\sigma_3$ = intermediate and minor principal stresses,

Pa = atmospheric pressure, and

$\alpha$ = the modulus exponent may be obtained from triaxial tests conducted at different confining pressure.

In the non-linear elastic analysis, the forces due to full excavation have been applied directly. Step- by- step excavation has not been considered. Secant modulus approach has been employed in the analysis, in which total force is applied in the first iteration and then secant modulus is modified in subsequent iterations according to the state of stress at a Gaussian point. The limitation of the program is that it is not applicable to non-linear failure cases of the rock mass. In the non-linear analysis, which would be more realistic, the sequence of excavation and the stress path may be incorporated. The program is being extended for the simulation of excavation sequence.

## 4. MAIN FEATURES OF SOFTWARE

The general purpose software ASARM (Analysis of Stresses in Anisotropic Rock Masses) has been developed for analysis of rock engineering problems with capability to simulate most of the problems associated with the geological discontinuities, like shear zones and fault zones. The 2- dimensional finite element software, developed for solving problems of plane stress, plane strain and axi-symmetric cases (Hinton and Owen, 1978), has been extended for non-linear elastic stress analysis of jointed rock masses in a 3-dimensional domain. The software may be useful for the analysis of slope stability, dam-foundation interaction problems and underground caverns.

The program consists of a MAIN program and 30 subroutines. The program structure is modular. The program has been written in FORTRAN. The geometry of the structure, the boundary conditions and the loadings are defined in global reference system.

The elements may be subjected to concentrated (point) loads, constant and variable pressure (traction) loading and gravity loading. The forces due to in-situ (initial) stresses, may also be applied. Multiple load conditions are allowed. Tensile stress has been considered as positive.

The program accommodates variation in material properties of the elements i.e. each element may have different material description. Isotropic and anisotropic continuum may be evaluated. The joint element facilitates modelling of interface between two different materials.

Systems composed of a large number of nodal points and elements may be analyzed. The capacity of the program depends mainly on the total number of nodal points in the system. There is no restriction, as such, on the number of elements or number of load cases. However, band-width, of the set of the equations to be solved, is restricted by the RAM available, whereas, the size of the problem which may be accommodated depends on the space available on Hard-disk. Stiffness matrices of all the elements are generated and stored in a specific order and stored first before the solver comes into action. The solver does the job of assembly of element stiffness matrices and reduction of equation simultaneously to optimise on memory requirement.

The program performs non-linear elastic stress analysis subjected to static loads only. In the present version of the program, all computations are done in double precision only for better numerical accuracy.

The flow of logic in the program has been presented in the form of flow charts in Figs. 5 to 8.

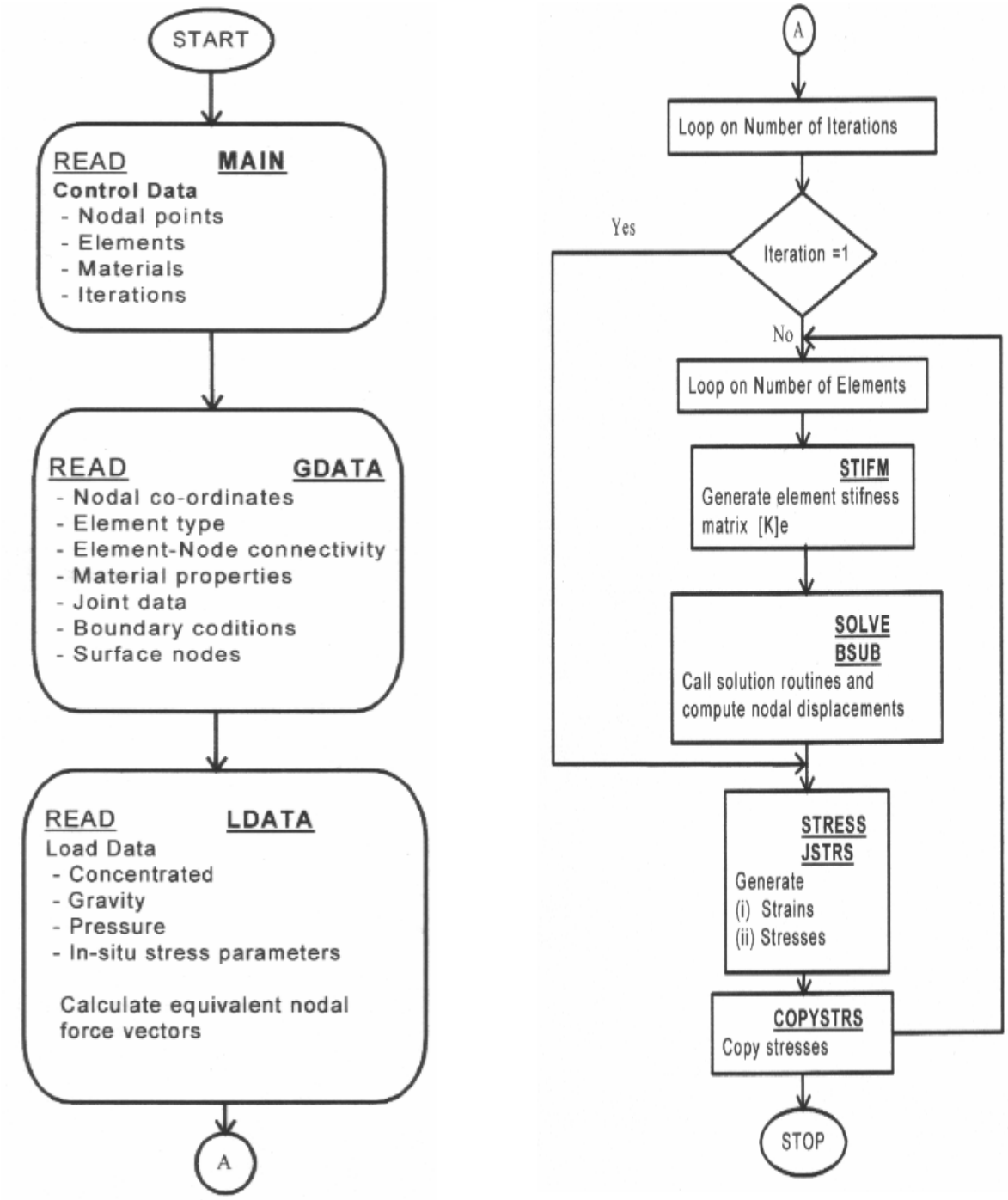


Fig. 5. Flow chart for finite element program for 3-dimensional non-linear elastic stress analysis

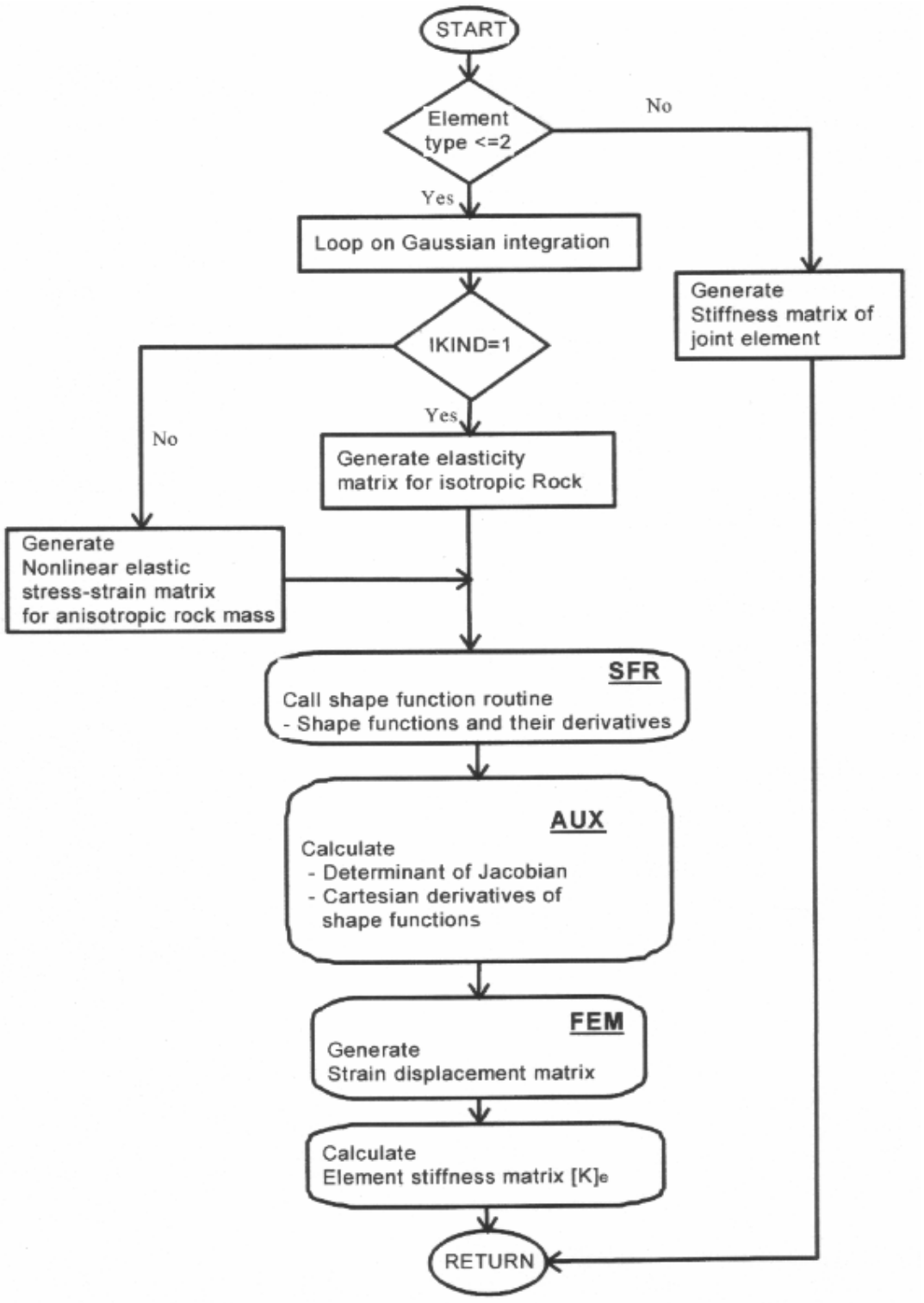


Fig. 6 – Flow chart for calculation of element stiffness matrix

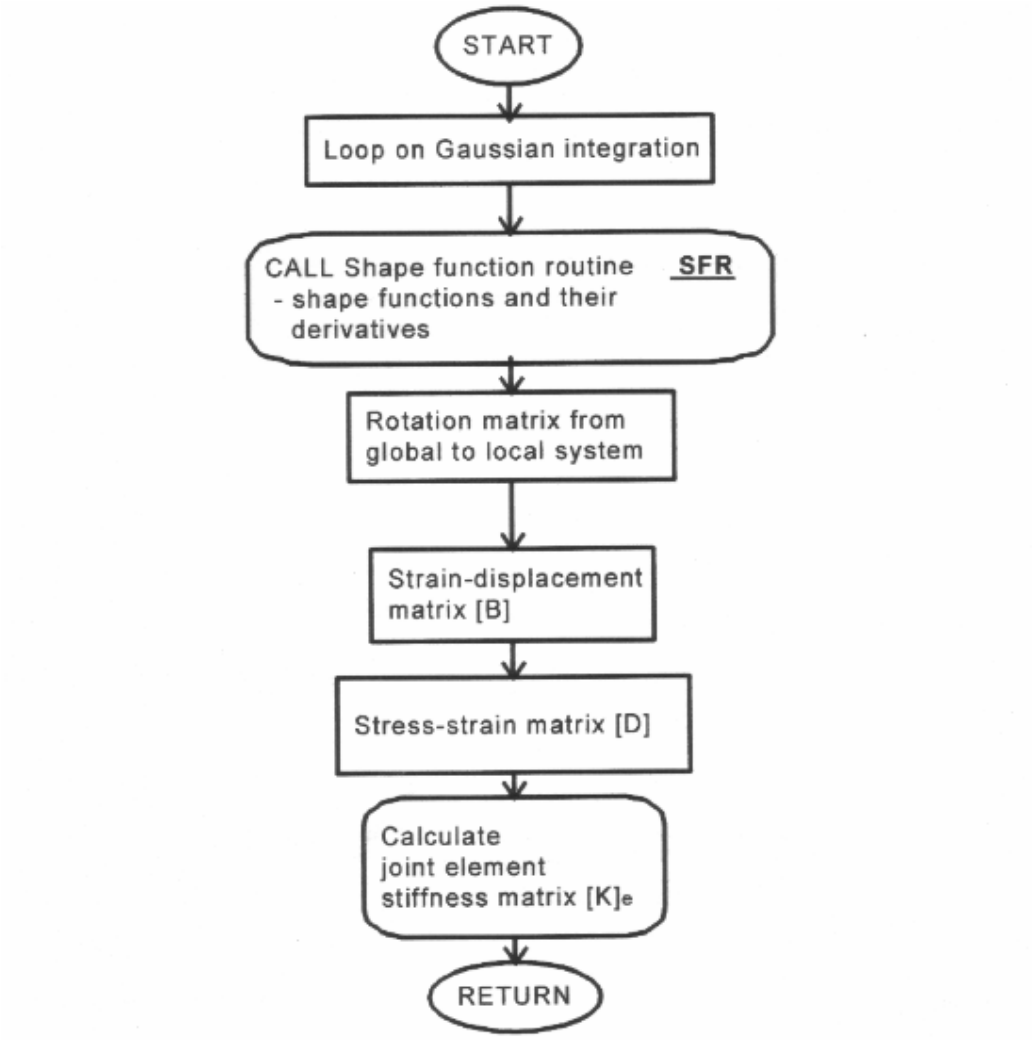


Fig. 7 - Flow chart for calculation of joint element stiffness matrix

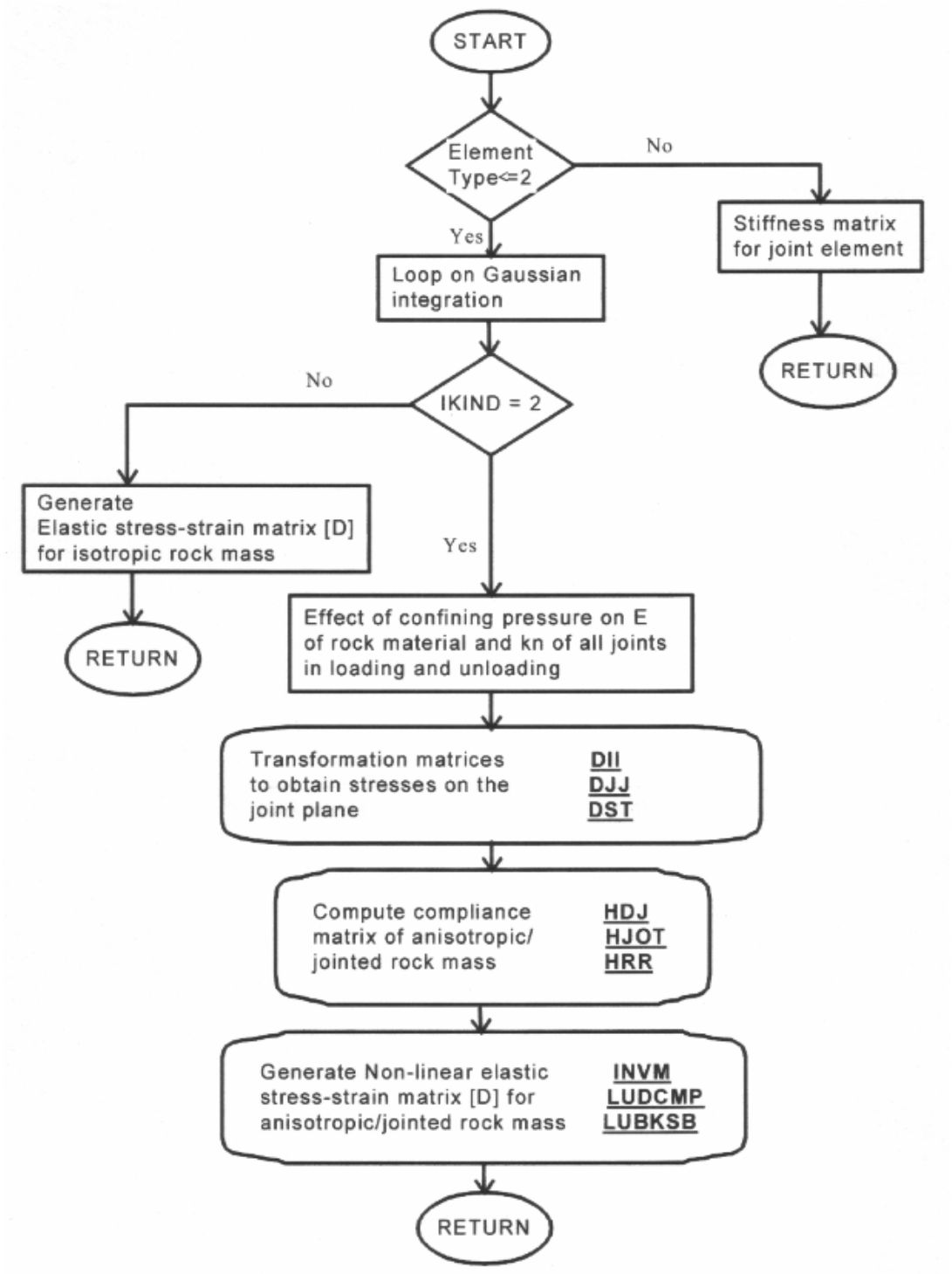


Fig. 8 - Flow chart for non-linear elastic stress-strain matrix [D] for anisotropic/jointed rock mass

### 4.1 Types of Elements Used

The present version of the program uses 20 - noded isoparametric brick element and 16 - noded joint element. The 20 - noded brick elements have been used in simulating the isotropic and anisotropic jointed rock masses, whereas, 16 - noded 3-D joint element has been used in the simulation of the characteristics of the interface between two different rock masses.

### 4.2 Material Characterization

Large scale discontinuities, such as joints and bedding planes, present in the rock mass make the rock mass behaviour a complex one. This complexity of material has been dealt with using an equivalent continuous material representative of the rock mass. An anisotropic continuum model based on the average influence of joints has been used in the present study.
In order to model the interface between two isolated and isotropic/anisotropic media, 16 - noded interface element has been employed. The material parameters $k_n$ and $k_s$ for this joint element also need to be given.

### 4.3 Load Cases

The program is especially suited to rock engineering problems, and therefore, has a provision for four different types of loading which may eventually be combined. The non-linear elastic analysis implies the need for several iterations for a complex loading in order to obtain deformations approaching reality.

Concentrated, gravity, pressure and initial stress loading use a consistent formulation as described earlier. The excavation simulation uses a special procedure described in subsequent section.

### 4.4 Stress Redistribution due to Excavation

The analysis of the excavation of an opening (Fig. 9a) is considered to be the sum of two separate cases as below (Fig. 9 b & 9 c).

(i) the given in-situ stress field and
(ii) the stresses due to release forces applied around the excavation.

The procedure is shown diagrammatically in Fig. 9a, 9b and 9c. The stress and displacement results obtained for cases (b) and (c) will be the same as those for (a), if boundaries are taken to be sufficiently far away from the excavation. However, it may be noted here that the displacements due to in-situ stresses have not been accounted for as those displacements had already taken place before excavation.

## 5. VALIDATION OF SOFTWARE

### 5.1 General

As the 3-D finite element software package developed in the present study for analysis of large underground cavities in jointed rock masses is quite general in nature, it is essential that the program is tested for its validation for solving some bench mark problems. Three typical problems have been chosen here from this point of view. These include:

(i) Analysis of a shallow tunnel excavated in an isotropic rock medium,
(ii) Analysis of a plate load test conducted on jointed rock mass and
(iii) Analysis of circular slip failure in a jointed rock.

Closed form analytical and/or a numerical solution are available for each of these three problems. Attempt has, therefore, been made here to solve these problems using the software and the results thus obtained have been compared with the available results to validate the software 'ASARM'.

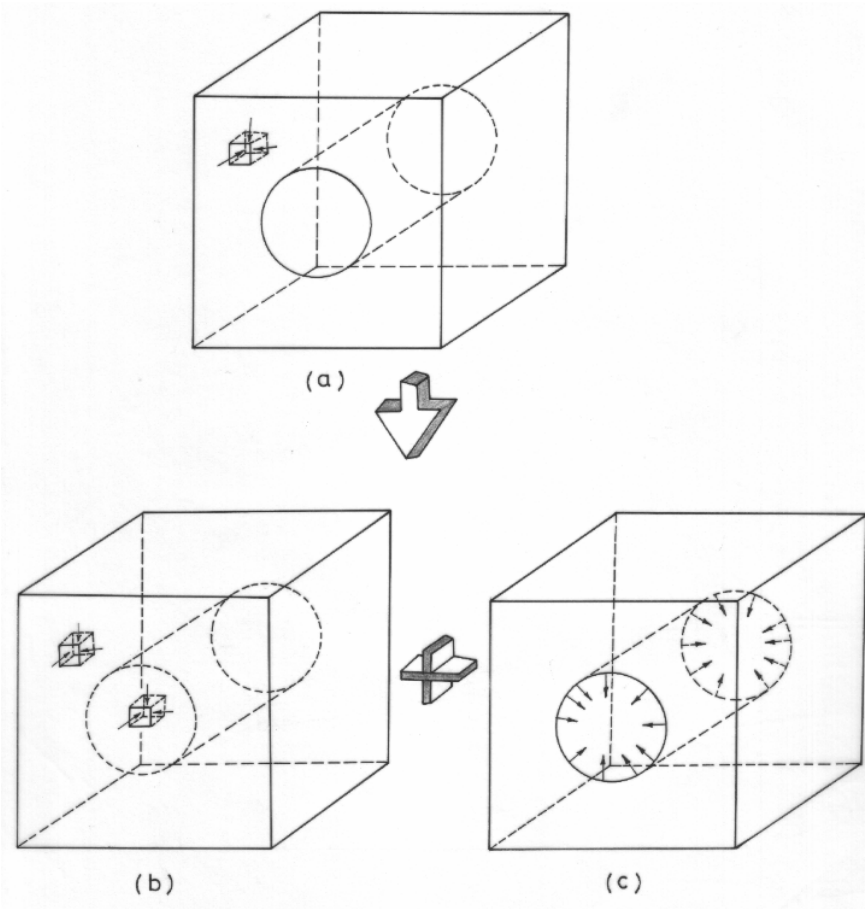


Fig. 9 - Schematic diagram simulating in-situ stress and excavation

## 5.2 Analysis of a Shallow Tunnel

### *5.2.1 Problem description and idealisation*

Case of a shallow tunnel excavated in an isotropic rock medium has been considered here for which closed form solution was presented by Jumikis (1983). The problem has also been solved numerically as a plane strain problem by Wang and Garga (1993) using 2-D finite element method. The problem consists of a tunnel with a radius of 2 m and excavated at a depth of 11 m below the ground surface. The geometry of the tunnel and the loads acting on it are shown in Fig. 10. The rock mass surrounding the tunnel is subjected to a vertical pressure intensity, $\sigma_v = \gamma H$ due to gravity and a lateral pressure intensity, $\sigma_h = [\mu/(1-\mu)]\ \gamma H$. The rock material properties used in the analysis are given in Table 1.

Table 1 - Material properties for analysis of shallow tunnel

| S. No. | Property | Symbol | Unit | Value |
|---|---|---|---|---|
| 1. | Young's Modulus | E | $kN/m^2$ | $5x10^7$ |
| 2. | Poisson's Ratio | $\mu$ | - | 0.25 |
| 3. | Unit Weight | $\gamma$ | $kN/m^3$ | 26.0 |

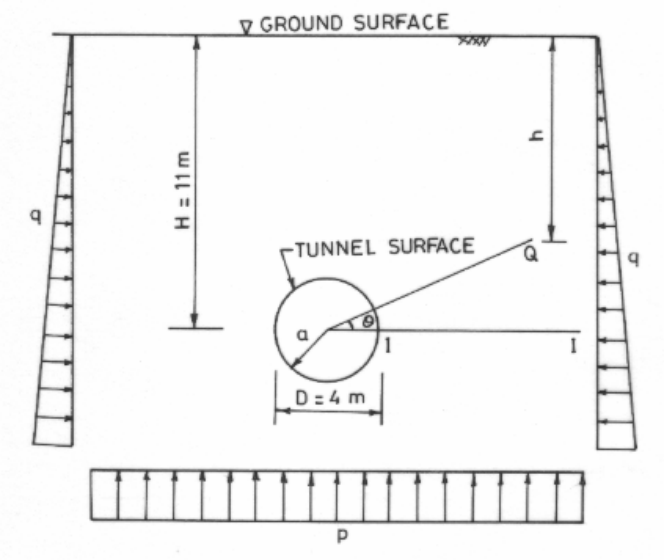


Fig. 10 - Geometry and loading at a shallow underground circular tunnel (After Jumikis, 1983 and Wang & Garga, 1993)

The rock mass surrounding the tunnel is treated as a linear elastic and isotropic medium. Figure 11a shows a two dimensional finite element discretization of the tunnel geometry, under the assumption of plain strain, as adopted by Wang and Garga (1993). In the present study, the tunnel along with the surrounding rock medium has been treated as a three dimensional body and Fig. 11b shows the corresponding finite element discretization in which it is clear that along the axis of tunnel, five slices, each with a width of 3 m, have been used. Rock mass extending to seven times the tunnel radius has

been considered in the plane of the tunnel, whereas it extends to 7.5 times the tunnel radius in the axial direction. Due to symmetry of both geometry as well as the loading, only half the geometry has been discretized. The finite element mesh consists of 245, 3-D brick element and 1427 nodes. The boundary conditions have been imposed on each boundary plane by restraining the displacement in the direction normal to the plane while permitting the in-plane displacement.

### *5.2.2 Tunnel behaviour*

The behaviour of the tunnel with respect to stresses, predicted on the basis of the proposed software, has been compared in Fig. 12 with that obtained by Jumikis (1983) using a closed form solution and by Wang and Garga (1993) using a numerical solution. Figure 12 shows the variation of both the horizontal ($\sigma_h$) and vertical ($\sigma_v$) stresses along the line passing through the horizontal axis of the tunnel. The horizontal stress is zero at the tunnel boundary, increases to a little over to 0.1 MPa upto a distance of 1.0 m beyond the tunnel periphery and then remains practically constant over horizontal extent under consideration and equals the lateral applied pressure intensity. The vertical stress is maximum at the tunnel periphery and is of the order of 0.8 MPa which equals about three times the applied vertical pressure intensity. The solutions of the other two authors have also been superimposed in the same plot and show a very good comparison.

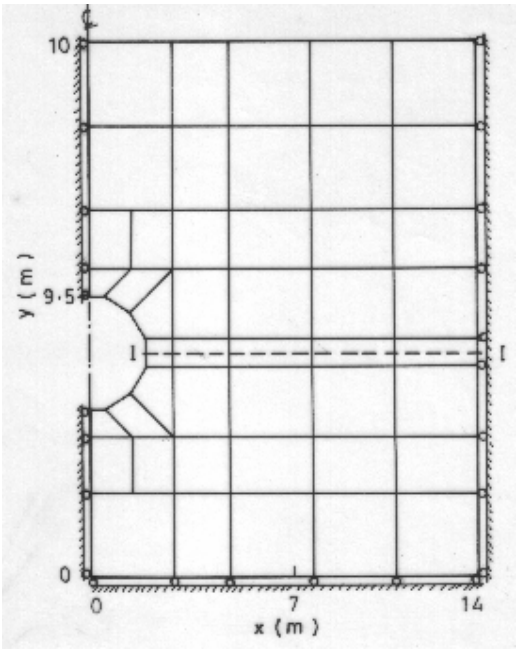


Fig. 11a – Two dimensional discretization of shallow tunnel
(after Wang & Garga, 1993)

Figure 13a shows the distribution of principal stress and orientation of the principal planes for the shallow tunnel. It shows that the stresses get redistributed in the vicinity of the tunnel. On comparison with similar results obtained by Wang and Garga (1993), it becomes clear from Fig. 13b that both principal stress and orientation of principal planes compared very well with those presented in Fig. 13a. The stresses plotted are at the C.G. of each element.

It has also been found that the stresses in the all the five slices of rock medium considered along the axial direction of tunnel are equal.

## 5.3 Analysis of a Plate Load Test on Jointed Rock Mass

### *5.3.1 Problem description and idealisation*

A problem of plate load test conducted by Iida and Kobayashi (1972) on jointed rock mass has been considered for analysis. Cai and Horii (1993) modelled the whole test numerically by using finite element method for jointed rock mass. The test problem consisted of a plate of diameter, 800 mm placed in a test pit at a depth of 100 m. The influence of depth has been considered in the analysis by applying an equivalent in-situ stresses. From practical stand point, the problem has been simulated as a plate resting on a block having dimensions, 10D x 10Dx 5D where D is the plate diameter. A single set of joints has been considered traversing through the rock mass. Taking the advantage of symmetry, only one-half of the block has been analysed. The plate has been simulated as equivalent square plate. Figure 14 shows the finite element mesh used in the present study.

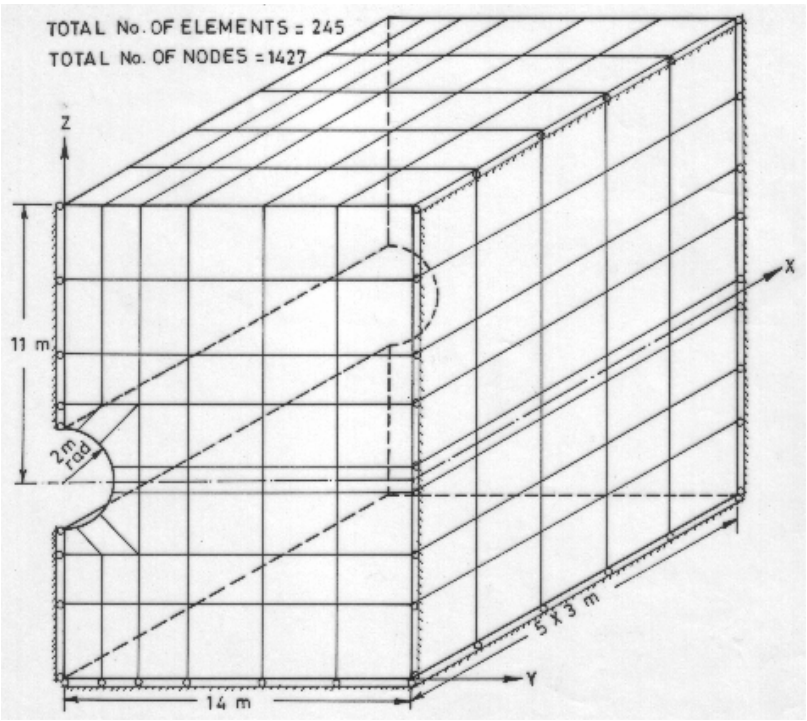


Fig. 11b – Three dimensional finite element mesh for tunnel (Present study)

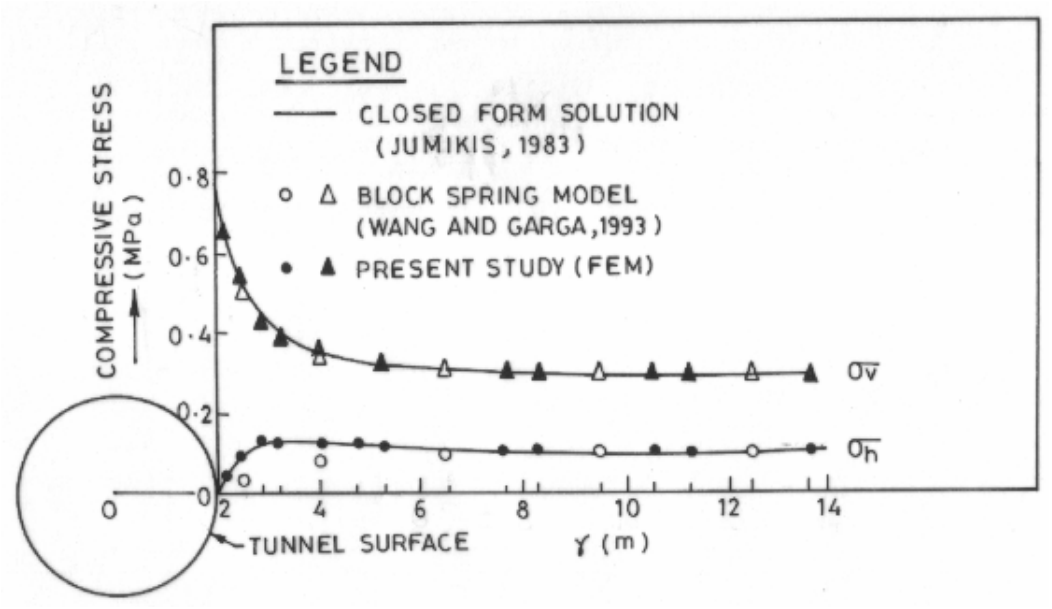


Fig. 12 - Horizontal and vertical stress distribution along axis I-I

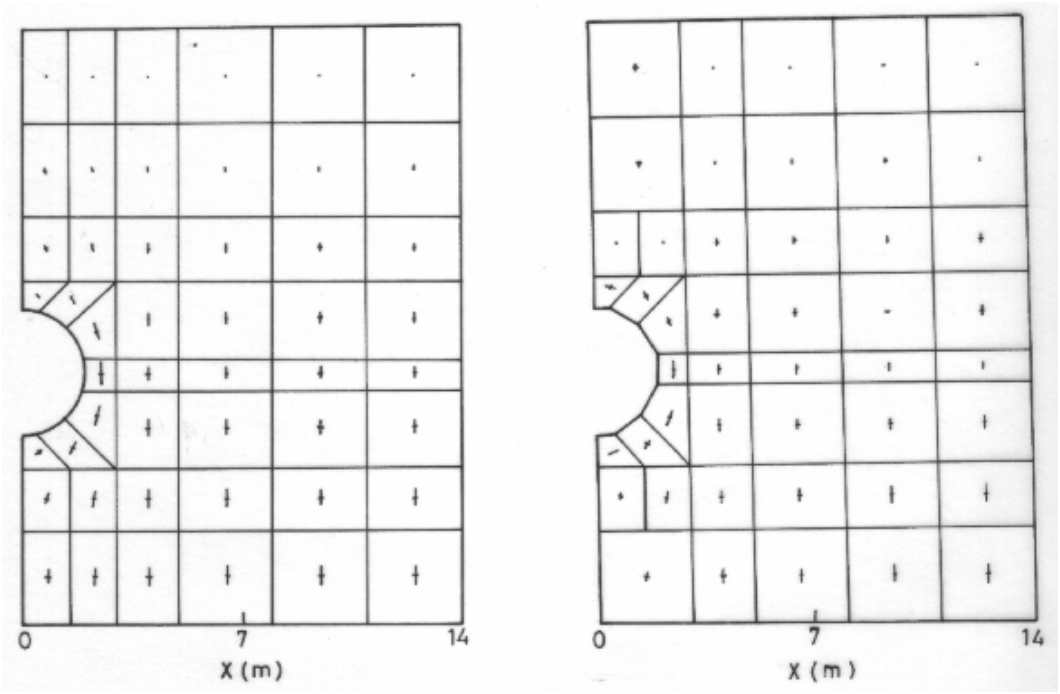


(a) Present study (b) After Wang & Garga, 1993

Fig. 13 - Principal stress and orientation of principal planes for shallow tunnel

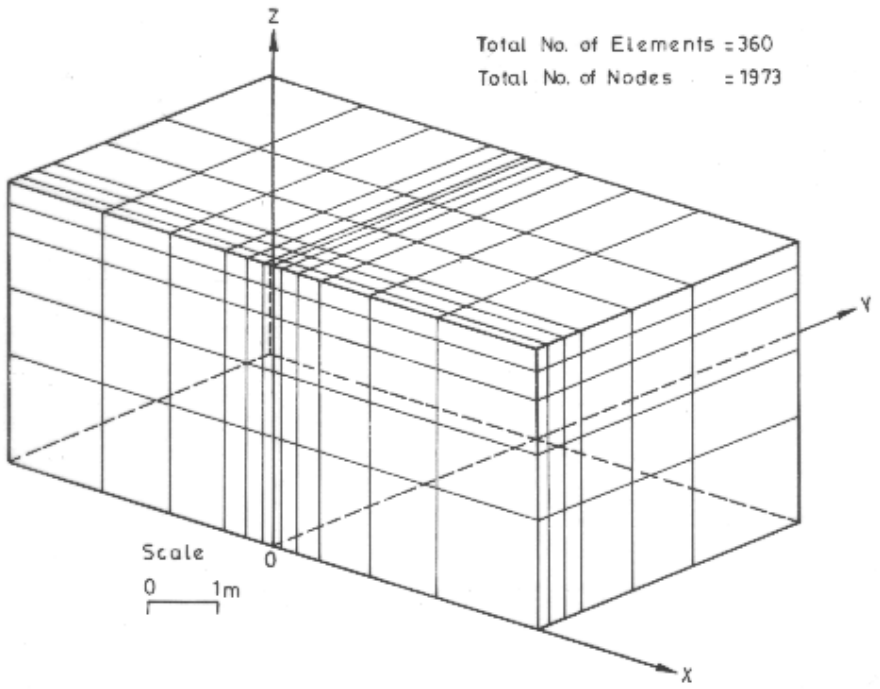


Fig. 14 - Finite element mesh used in 3-D analysis of plate loading test on jointed rock

The mesh consists of 360, 3-D brick elements and 1973 nodes. Boundary conditions were imposed by restraining all the nodes lying at the boundary in all three directions, those lying on the plane of symmetry have been restrained only in the Y-direction. The material properties of the rock mass used in the analysis are presented in Table 2.

Table 2 - Material properties for plate load test

| S. No. | Property | Symbol | Unit | Magnitude |
|---|---|---|---|---|
| 1 | Young's Modulus | E | $kN/m^2$ | $21.2x10^6$ |
| 2. | Poisson's Ratio | $\nu$ | $kN/m^3$ | 0.25 |
| 3. | Density | $\gamma$ | | 27 |
| 4. | Number of Joint Sets | - | | 1 |
| 5. | Dip of Joints | $\psi_j$ | | $40^o$ |
| 6. | Dip direction of Joints | $\alpha_j$ | | $0^o$ |
| 7. | Joint Spacing | | | 0.15 m |
| 8. | Normal Stiffness of Joints | $k_{nl}$ | $kN/m^3$ | E/0.6, E/0.5, E/0.4 |
| 9. | Shear Stiffness | $k_s$ | $kN/m^3$ | $k_{nl}/10$ |

### *5.3.2 Numerical results and comparison*

In the present study, the 3-D finite element analysis of plate load test data was carried out for three different values of the normal stiffness of joints in loading (Table 2). In order to simulate the experimental data of Iida and Kobayashi (1972) in a realistic manner (Fig. 15), it is essential to perform a completely non-linear analysis including both loading and unloading situations. Similarly the experimental data also show that there are three cycles

of loading and two cycles of unloading. An incremental elasto-plastic analysis can also simulate the effect of these loading and unloading cycles and the resulting accumulated displacement. However, the software developed in the present study can take into account only linear and non-linear elastic situations. The unloading cycles have therefore not been simulated in the present study and once a linear analysis is performed, it can be done for only one cycle of loading.

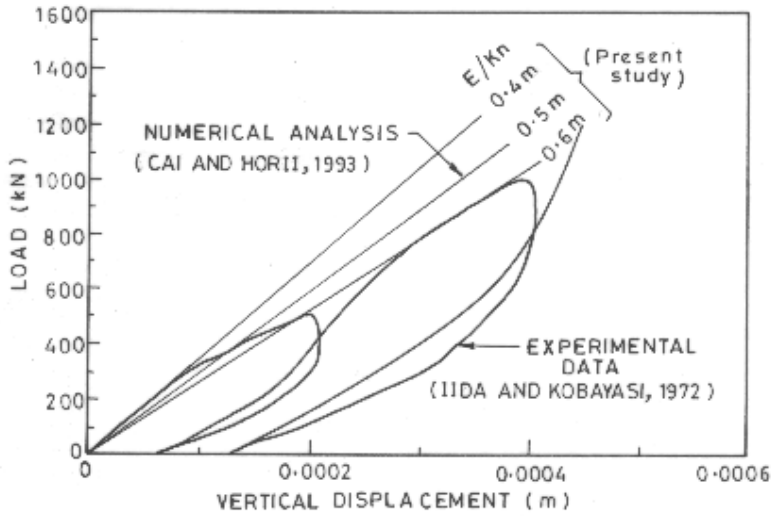


Fig. 15- Relations between the vertical load and the vertical displacement at the plate center

Figure 15 shows load versus vertical settlement plot obtained in the present study for three values of normal stiffness of the rock joints and comparison with numerical results of Cai and Horii (1993). The experimental data of Iida and Kobayashi (1972) has also been superimposed in the same figure. Numerical results of the present study and those of Cai and Horii (1993) do agree with the experimental ones for the loading cycle and for the case when $E/k_n$ equals 0.5, results obtained in the present study coincide with those of Cai and Horii (1993). It is heartening to note that Singh and Goel (1982) have found $E/k_n$ to be about 0.6 m for continuous unweathered joints.

## 5.4 Analysis of a Circular Slip in a Jointed Rock

### *5.4.1 Problem definition*

The basic purpose of the joint element is to permit relative slip at the interface of two material blocks, made up of same or different materials. The software developed has also been tested for this feature of the joint element. A case of circular slip in a rock body has been analysed for this purpose. The finite element mesh used to model the system has been shown in Fig. 16. The mesh consists of six 20 - noded brick elements, three 16 noded joint elements and 88 nodes. Boundary conditions have been imposed by restraining the base of lowermost three elements. The upper block is subjected to an uniformly distributed load of 100 $kN/m^2$ as shown in Fig. 16.

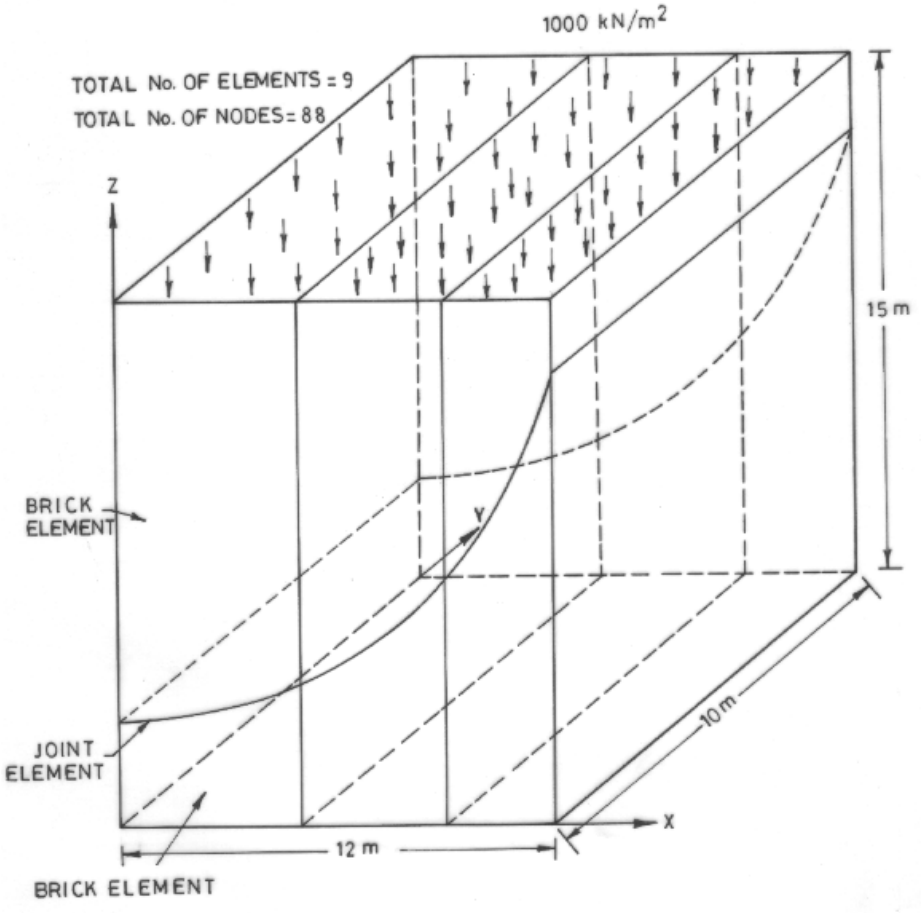


Fig. 16 - Finite element mesh for modelling circular slip

The system has been analysed for two different properties of joints, namely, i) low shear modulus, permitting the slip, and (ii) very high shear modulus simulating a welded contact between two joint planes. Material properties used in the analysis are presented in Table 3.

Table 3 - Rock material and rock joint properties

| S. No. | Material Property | Symbol | Units | Magnitude |
|---|---|---|---|---|
| I. | Rock Material | | | |
| 1. | Young's Modulus | E | $kN/m^2$ | $2.0x10^7$ |
| 2. | Poisson's ratio | $\nu$ | -- | 0.2 |
| II | Joint Element | | | |
| | (Low Shear Modulus) | | | |
| 3. | Shear Stiffnesses | $k_{s1}$, $k_{s2}$ | $kN/m^2$ | 2000.0 |
| 4. | Normal Stiffnesses | $k_n$ | $kN/m^2$ | $4.0 x10^7$ |
| III | Welded Contact | | | |
| | (High Shear Modulus) | | | |
| 5. | Shear Stiffnesses | $k_{s1}$, $k_{s2}$ | $kN/m^2$ | $2.0 x10^7$ |
| 6. | Normal Stiffnesses | $k_n$ | $kN/m^2$ | $2.0 x 10^8$ |

### *5.4.2 Numerical results*

The results obtained from the analysis have been presented in Fig. 17a for the case of low shear modulus and in Fig. 17b for the case of high shear modulus (welded joint). It may be observed (Fig. 17a) in the case of low shear modulus that the upper part of the block has slided as a rigid block along the joint surface under the applied loads. In the case of welded contact, no slip has been observed. The shear stresses along the slip surface of joint planes have been computed as 347.2 to 347.9 kN/m$^2$. By Swedish circle method (Fellenius, 1926), the shear stresses are obtained as 348.0 kN/m$^2$ when the rock mass has been considered as purely cohesive material, i.e. ($\phi$ = 0). Therefore the shear stresses obtained in the present study are in order.

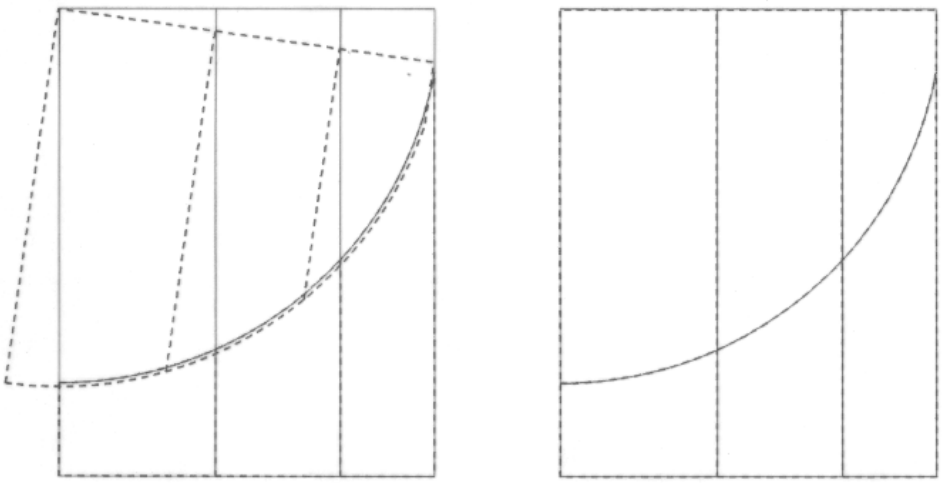

(a) Low shear modulus (b) High shear modulus

Fig. 17 - Displacements of top block

It is worth mentioning here that the purpose of this test case was to check whether the joint element is working or not. Therefore in order to test curvilinear joint element circular failure was considered. However the program may be checked for wedge failure also. Further when very low shear stiffness was considered, the slip occurred along the joint plane therefore the results were compared with ($\phi$ = 0) condition.

## 6. CONCLUSIONS

Based on finite element methodology, software for 3-dimensional linear and non-linear elastic stress analysis of large underground openings i.e. caverns has been developed. The program possesses the versatility associated with the material, geological configuration and geometry. Constitutive equations for the anisotropic rock mass and 3-Dimensional joint element have also been incorporated. It may be noted that the software may also be employed for the problems of

(i) abutment analysis and
(ii) dam-foundation interaction.

The program of this nature has to be used with great care in analysing practical design problems since there is seldom sufficient reliable information on rock mass characteristics and in-situ-stress field. However, it can be used for carrying out a number of parametric studies in which the various input assumptions are varied over their maximum credible range in order to determine their influence upon the calculated results. In this way, a range of possible solutions could be obtained and these can be used as an aid to practical common sense in reaching design decisions.

An attempt has been made for validation of the 3-D finite element software developed as part of this study. Three problems have been chosen for the purpose. Barring the limitations of the program, it can be reasonably argued that the software may be successfully used for further analysis, especially the powerhouse caverns of the hydro-power projects.

***References***

Bathe, K.J. (1982). Finite Element Procedures in Engineering Analysis, Prentice Hall, London, p. 735.

Cai, M. and Horii, H. (1993). A Constitutive Model and FEM Analysis of Jointed Rock Masses, Int. J. of Rock Mech. Min. Sci. & Geomech. Abstr., Vol. 30, No.4, pp. 351-359.

Goodman, R.E., Taylor, R. and Brekke, T.L. (1968). A Model for the Mechanics of Jointed Rock, J. Soil Mech., Found. Engg. Div., ASCE, Vol. 94, No. SM3, pp. 637-659.

Fellenius, W. (1936). Calculation of Stability of Earth Dams, Trans. 2nd Congress on Large Dams.

Hinston, E. and Owen, D.R.J. (1978). Finite Element Programming, Academic Press.

Iida, R. and Kobayashi, S. (1972), Measurement of Mechanical Response of Rocks at a In-situ Loading Test, Technical notes in Civil Engg., Resh. Instt. of Civil Engg., Ministry of Construction in Japan, Vol. 14, pp. 392-396.

Janbu, N. (1963). Soil Compressibility as Determined by Odometer and Triaxial Tests, European Conf. Soil Mech. Foundn. Engg., Wiesbaden, Vol. 1, pp. 19-25.

Jumikis, A.R. (1983). Rock Mechanics, 2nd Ed. Transtech. Publications, Clansthal - Zellerfeld, Germany, pp. 220-226.

Samadhiya, N.K. (1998). Influence of Anisotropy and Shear Zones on Stability of Caverns, Ph.D. Thesis, Department of Civil Engineering, University of Roorkee, Roorkee, p. 334.

Singh, B. and Goel, P. K. (1982). Estimation of Elastic Modulus of Jointed Rock Masses From Field Wave Velocity, R.S. Mittal Commemorative Volume on Engineering Geosciences, Ed. B. B. S. Singhal, Sarita Prakashan, India, pp. 156-172.

Wang, B. and Garga, V. K. (1993). A Numerical Method for Modelling Large Displacements of Jointed Rocks - I Fundamentals, Canadian Geotech. Journal, Vol. 30, pp. 96-108.

Zienkiewicz, O.C. and Taylor, R.L. (1992). The Finite Element Method, Chapter 4, McGraw Hill, 4th Edition.